Temporal change and flow velocity estimation of Patseo glacier, Western Himalaya, India

K. K. Singh[1,*], D. K. Singh[1,2], H. S. Negi[1], A. V. Kulkarni[3], H. S. Gusain[1], A. Ganju[1] and Babu Govindha Raj K.[4]

[1]Snow and Avalanche Study Establishment, Chandigarh 160 036, India
[2]PEC University of Technology, Chandigarh 160 012, India
[3]Divecha Centre for Climate Change, Indian Institute of Science, Bengaluru 560 012, India
[4]Indian Space Research Organization, Head Quarters, New BEL Road, Bengaluru 560 231, India

In the present study we estimate the velocity and thickness of the Patseo glacier, Himachal Pradesh, India. The average velocity of the glacier was estimated as ~5.47 m/year using co-registration of optically sensed images and correlation (COSI-Corr) method. The glacier thickness was found to vary between 12 and 278 m, with an average value 59 m. The total glacier ice volume was estimated as ~15.8×10^7 m^3, with equivalent water reservoir of ~14.5×10^7 m^3. Ground penetrating radar (GPR) surveys were conducted during 2004 and 2013 for validation of the estimated glacier thickness. The glacier thickness estimated using COSI-Corr method was found to be in agreement with GPR-retrieved glacier thickness (RMSE = 4.75 m; MAE = 3.74 m). The GPR profiles collected along the same geographic locations on the glacier during 2004 and 2013 showed a reduction in ice thickness of ~1.89 m, and thus resulting in an annual ice thickness decrease of ~0.21 m. The glacier area was estimated for 2004 and 2013 using LISS IV satellite data and found to be ~2.52 and ~2.30 sq. km respectively. This shows an annual reduction of ~0.024 sq. km in glacier area. The total annual loss in glacier ice volume was estimated as ~4.55×10^5 m^3. This loss in the glacier ice volume of the Patseo glacier is supported by the snow and meteorological observations collected at a nearby field observatory of Snow and Avalanche Study Establishment (SASE). The climate data collected at SASE meteorological observatory at Patseo (3800 m), between 1993–94 and 2014–15 showed an increasing trend in the mean annual temperature and a decreasing trend in winter precipitation.

Keywords: Glaciers, ground penetrating radar surveys, velocity and thickness estimation, winter precipitation.

Introduction

GLACIERS are the most visible indicators of the effects of climate change. Recent studies in glaciology indicate an increase of glacier mass loss all over the world, including the Indian Himalaya[1–4]. It is difficult to assess the glacier thickness information from the rugged Himalayan glaciers. However, this information and glacier ice thickness distribution are essential in various hydrological studies.

Remote sensing satellite data-based techniques are widely used to study the glacier dynamics mainly for the estimation of glacier surface velocity. Several researchers have reported the use of synthetic aperture radar (SAR) data for velocity estimation[5–7]. Though acquisition of SAR data is independent of weather conditions (clouds and rainfall), the loss of coherence due to melting of snow and glaciers, invisibility of steep terrain glaciers due to the impact of incidence angle, etc. are some of the limitations.

Optical satellite data-based image correlation is another promising method to estimate the displacement of an object over a period of time. Different correlation techniques such as cross-correlation in spatial and frequency domains, sub-pixel phase correlation and orientation correlation were used to estimate the glacier surface velocity[8–10]. Co-registration of optically sensed images and correlation (COSI-Corr) is used extensively for estimating the speed of glaciers and also to analyze their spatio-temporal variations over a long time[11–13].

In the present study surface velocity and thickness of the Patseo glacier located in the Great Himalaya range are estimated. Velocity map of the glacier is generated by applying COSI-Corr technique on Landsat satellite data of 2014 and 2015. Surface velocity map along with slope information is used to generate thickness map of the glacier. The thickness values retrieved from the thickness map for some of the geographic locations are validated using ground penetrating radar (GPR) thickness data measured for the same locations in the glacier. The GPR survey of the glacier was conducted in 2004 and 2013. During these surveys, measurements were carried out at the same locations in the glacier. The GPR data collected during 2004 and 2013 were further used for estimation of temporal change in glacier thickness. The areal change in the glacier between 2004 and 2013 was also estimated using LISS IV satellite data.

*For correspondence. (e-mail: kamal.kant@sase.drdo.in)

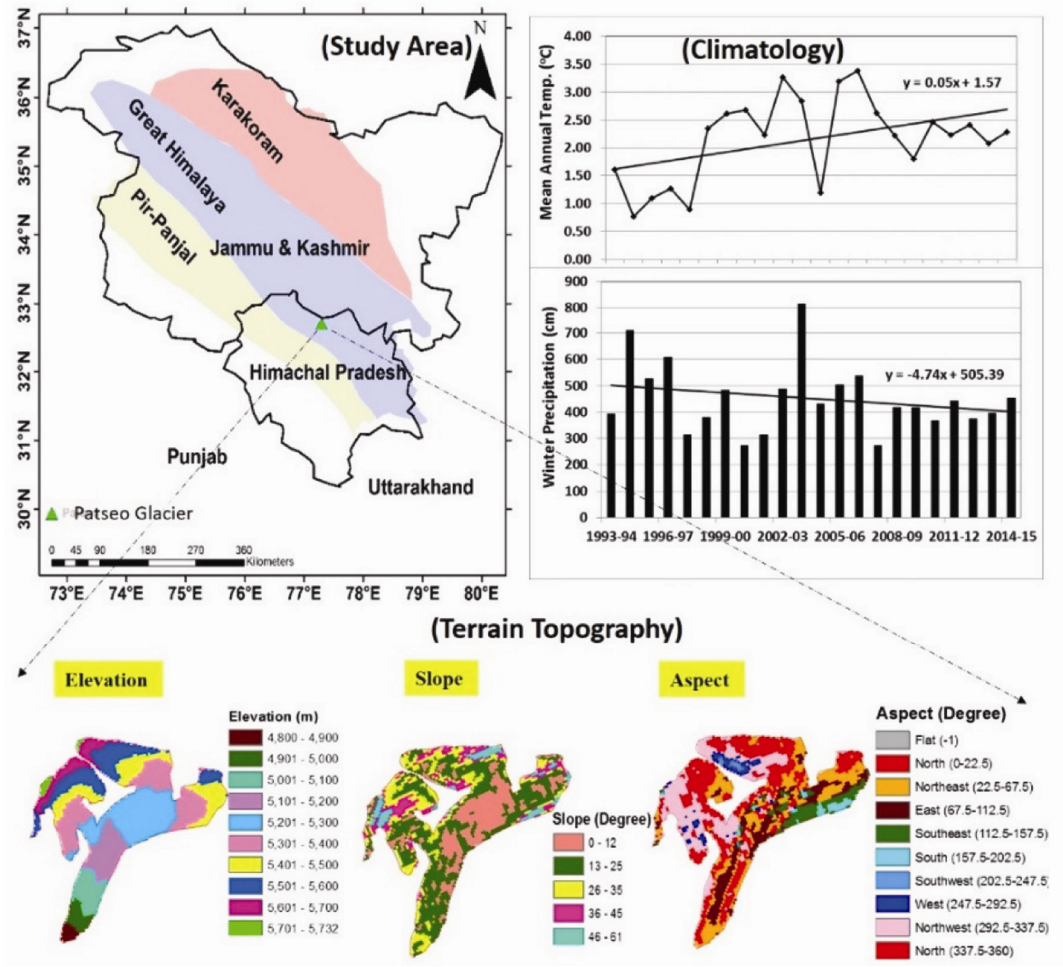

Figure 1. Study area (Patseo region in the Great Himalayan range), topography and climatology.

Study area and climatology

The Patseo glacier (32°46′02″N, 77°82′26″E) lies in the Bhaga river basin in the Great Himalayan range. The length and area of the glacier are ~3.5 km and ~2.52 sq. km respectively. The glacier is located within the elevation range 4820–5724 m amsl, with mean elevation 5298 m and orientation towards north-east direction (Figure 1). The snow and metrological data collected from a nearby observatory of Snow and Avalanche Study Establishment (SASE) were considered as a representative in the present study. The manually collected data between 1993 and 2015 were analysed to generate the climatology of the area. From the analysis, the mean annual temperature was observed to be increasing at ~0.05°C/year; however, winter precipitation was found to be decreasing at the rate of ~4.74 cm/year (Figure 1). For analysis of climate data, we have carried out Mann–Kendall test to check the significance of the linear trends and observed that for both mean annual temperature and winter precipitation, the trends were not significant. Negi *et al.*[14] also found an overall increasing trend in the mean annual temperature and a decreasing trend in winter snowfall (November to April) in the area during 1983–2011.

Data used and methodology

In the present study, Landsat 8, Panchromatic data (2014 and 2015) of 15 m spatial resolution along with advanced spaceborne thermal emission and reflection radiometer (ASTER) GDEM with spatial resolution 30 m have been used to estimate surface velocity of the glacier. Table 1 provides details of the datasets used for the study.

The area-wise change in the glacier between 2004 and 2013 was estimated using LISS IV satellite having spatial resolution of 5.8 m. Figure 2 shows the overall methodology adopted in the present study.

Estimation of glacier surface velocity

COSI-Corr method developed by Leprince *et al.*[15] was used to estimate the glacier surface velocity by performing

the sub-pixel correlation among the satellite images. This COSI-Corr module is freely available and can be downloadable from http://www.tectonics.caltech.edu. In this technique a frequency correlator was used to correlate two selected time-series images. A 32 × 32 pixel sliding window with a step size of two pixels was considered to perform the correlation. This process resulted in three output images, i.e. east–west (EW) displacement, north–south (NS) displacement and signal-to-noise ratio (SNR). Due to the step size (2) and resolution (15 m for Landsat data), we could generate these images at 30 m spatial resolution. Further, pixels having SNR <0.9 were discarded and the EW and NS displacements were used to estimate the net displacement (R_{dis})

$$R_{dis} = \sqrt{NS^2 + EW^2}. \quad (1)$$

The annual surface velocity (U_S) of the glacier was estimated using the displacement data and the difference in acquisition dates of the two satellite images used in the analysis.

$$U_S = \frac{R_{dis} \times 365}{\text{Number of days bewteen two used images}}. \quad (2)$$

Table 1. Description of datasets used for the analysis

Data	Date of acquisition	No. of bands	Resolution (m)
Landsat 8	28 September 2014	8	15
Landsat 8	1 October 2015	8	15

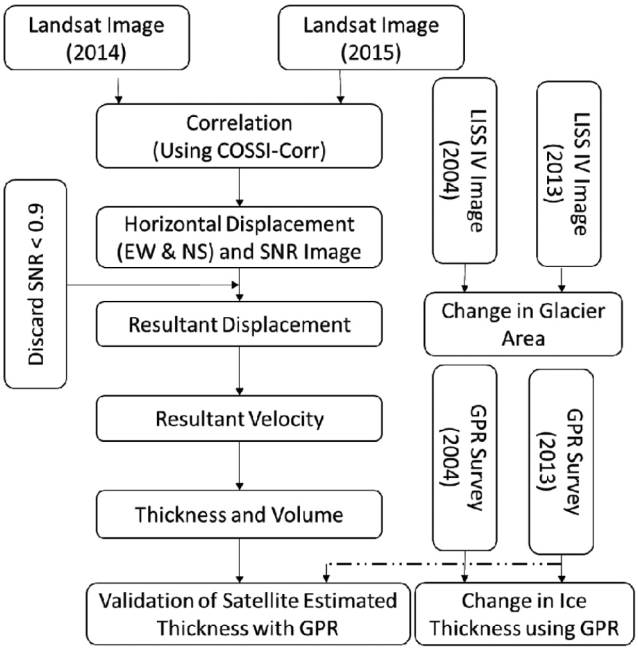

Figure 2. Flowchart of the methodology adopted.

Estimation of glacier depth using satellite data

Glacier thickness (H) was estimated as follows[13]

$$H = \sqrt[4]{\frac{1.5U_S}{Af^3(\rho g \sin\alpha)^3}}, \quad (3)$$

where U_S is the glacier surface velocity, ρ the ice density (900 kg m^{-3})[16], g the acceleration due to gravity (9.8 m s^{-2}) and f is a scale factor, i.e. ratio between the driving stress and basal stress along a glacier, and the range for this scale factor is 0.8 to 1 for temperate glaciers. In the analysis we used $f = 0.8$ (ref. 17). ASTER GDEM at 30 m contour intervals was used to estimate the glacier slope (α). This interval was chosen so that the surface slope could be averaged over a reference distance that is about an order of magnitude larger than the local ice thickness[18,19]. The glacier depth information was generated for each 30 m interval. These depth values were then plotted spatially to create the thickness map of the glacier. This map was smoothened using focal filter to deliver a more realistic ice-depth map of the glacier.

Figure 3. Field photographs of ground penetrating radar (GPR) survey at the Patseo glacier during (***a***) 2004 and (***b***) 2013.

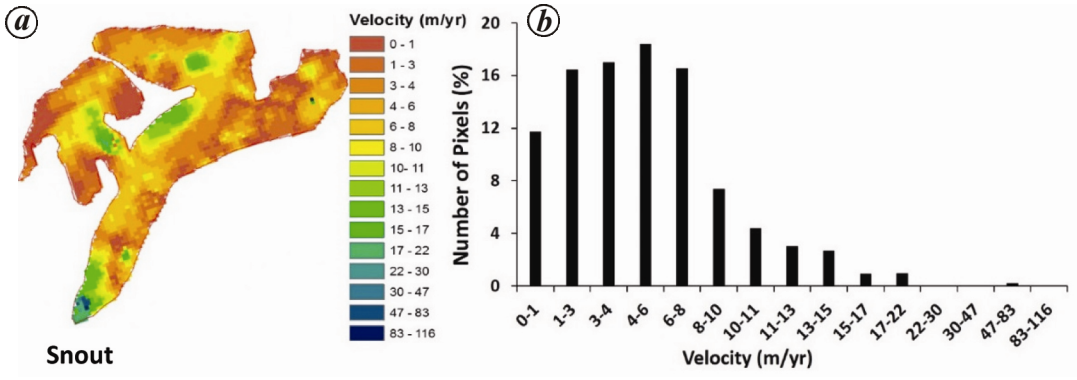

Figure 4. Surface velocity map (***a***) and velocity histogram (***b***) of the Patseo glacier (2014–15).

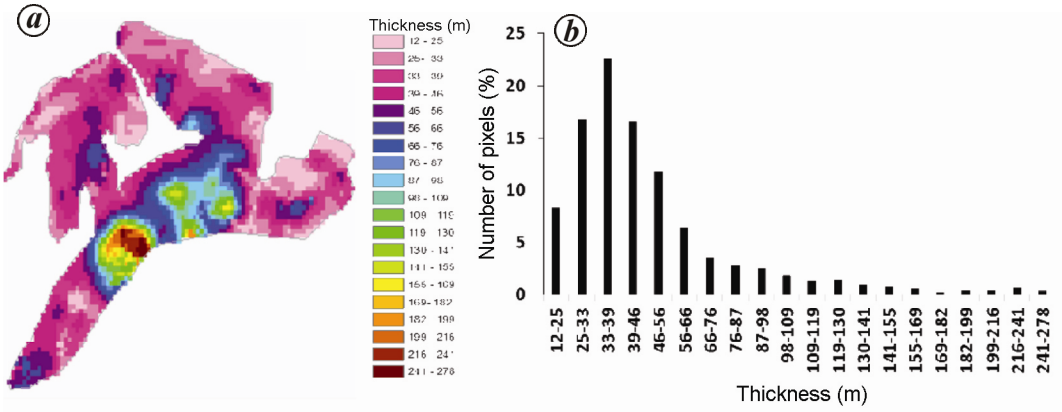

Figure 5. Ice thickness distribution map (***a***) and thickness histogram (***b***) of Patseo glacier (2014–15).

Estimation of glacier depth using GPR

In the present study GPR antennas of frequency 50 (Ramac GPR from Mala Geoscience, Sweden; www.malagas.com) and 40 MHz (Radarteam, Sweden; www.radarteam.se) were used during 2004 and 2013 respectively (Figure 3), for depth estimation at the Patseo glacier.

The 50 MHz antenna used with Ramac GPR is unshielded (bistatic) in nature with transmitter and receiver distance being about 2 m. GPR profiles were collected in time mode using long time-windows (600–1000 ns). Data were stored in 16-bit integer raw data format and further transferred from control unit to laptop. Post-processing of the data was done using Ground Vision software. The display of data was enhanced in terms of dynamical range by applying a top mute of first arrival corresponding to the direct wave. To remove the dark current, DC filter was used and further to compensate the loss in data due to spreading and attenuation, the time gain filter was applied.

The Radarteam GPR system with 40 MHz monostatic antenna was also used to collect the glacier thickness profiles. Here too the GPR profiles were collected in time mode. Post-processing of the GPR data was carried out using Reflex 2D Quick software. To enhance the weak signals, a gain function was used in both pre- and post-processing of radar profiles. Filters such as subtract DC shift, bandpass butterworth (lower cut-off 10 MHz and upper cut-off 120 MHz), and background removal were applied on the GPR data during post-processing.

Velocity of propagation of radio waves in ice is essential for the interpretation of GPR profiles collected from the glacier. The velocity (v) at which the electromagnetic (EM) wave travels through any medium can be estimated as follows

$$v = c/(\varepsilon_r)^{1/2}, \tag{4}$$

where c is the speed of light (3×10^8 m/s) and ε_r is the dielectric constant of the medium.

EM wave velocity is greatest in vacuum and decreases with increasing dielectric constant. In the present study GPR profiles were processed using EM wave velocity ~0.168 m/ns as reported for the ice media[20,21]. The EM wave velocity was further used to calculate the expected two-way travel time (TWT) of reflection as follows

$$\text{TWT} = 2d/v, \tag{5}$$

where d is the depth of the glacier.

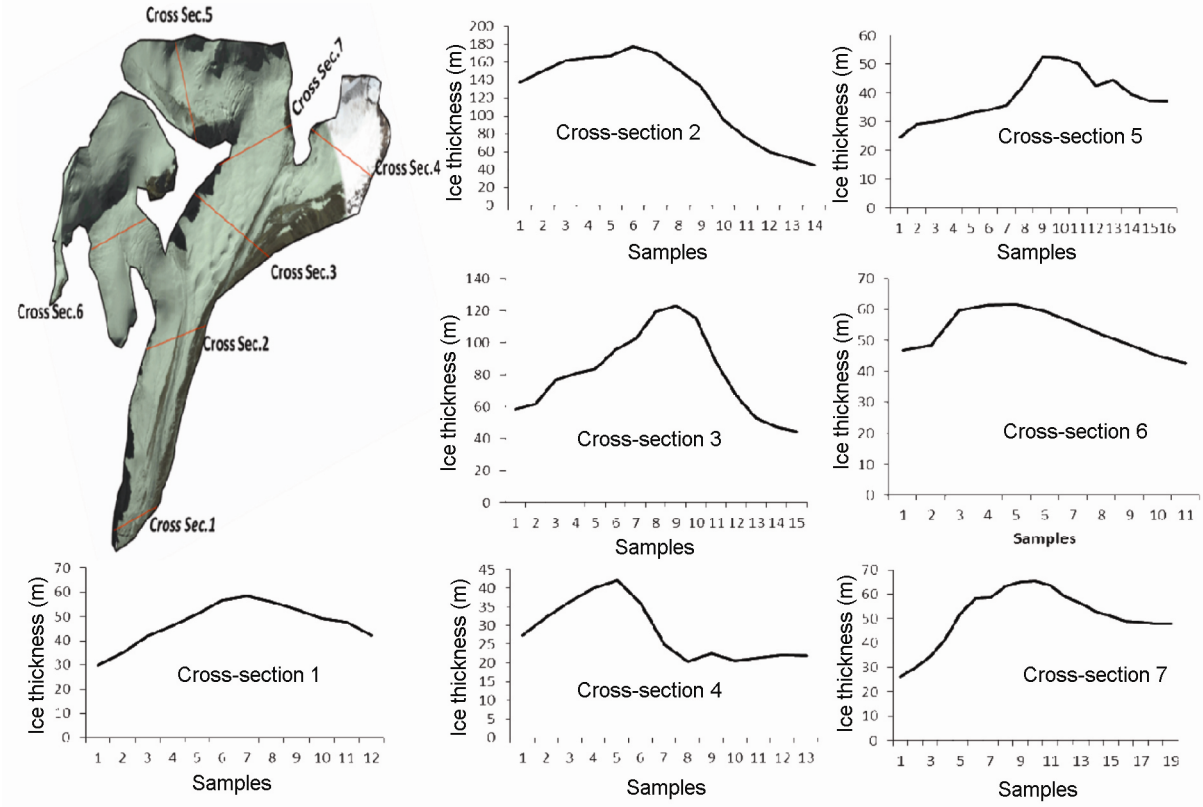

Figure 6. Ice-thickness distribution of Patseo glacier along cross-sectional (1–7) profiles.

Estimation of uncertainty in glacier mapping

Uncertainty in glacier mapping can be numerically estimated as follows[22]

$$\text{Mapping error} = N * \frac{A}{2}, \tag{6}$$

where N is the number of pixels along the glacier boundary and A is the area of a pixel.

Results and discussion

Figure 4 *a* and *b* shows the surface velocity map of the Patseo glacier and its histogram respectively. The surface velocity of the glacier ranged from 1 to 116 m/year with average ~5.47 m/year. Figure 4 *a* shows that the glacier surface velocity varies between 11 and 47 m/year near its snout. These high values of velocity near the snout in comparison to the average velocity values may be attributed to the higher slopes near the snout region. Figure 4 *b* shows that for most (more than 98%) of the glacier, the velocity values remain below 30 m/year.

Figure 5 *a* and *b* shows the ice-thickness distribution map of the Patseo glacier and its histogram respectively. The glacier ice thickness ranged from 12 to 278 m, with an average value of 59 m.

The maximum ice thickness value (278 m) was observed in the central part of the main trunk. Ice depth varied from 46 to 87 m near the snout of the glacier. The histogram shows that most of the pixels in the thickness map have values ranging from 12 to 169 m.

Figure 6 is a plot of seven ice-thickness profiles at different cross-sections on the glacier. Ice thickness was higher in the middle compared to either side of the glacier. The maximum ice thickness was observed in cross-sections 2 and 3 varying from 44 to 178 m. The lower values of slope along these cross-sections may be one of the reasons for higher values of ice thickness. Ice thickness values were observed to be comparatively less along profiles 1, 4–7. The higher slopes in these profiles result in these thickness values which vary from 20 to 65 m.

The ice-thickness map was also used to obtain the bed topography of the glacier (Figure 7). For this, a profile was drawn along the centre of the glacier with 34 observation points (Figure 7 *a*). The surface topography of the glacier was plotted using ASTER DEM. Here the difference between the glacier surface elevation and bed topography elevation depicts the glacier ice depth. Figure 7 *b* shows that up to a distance of ~1 km (observation point 11) from the snout, ice thickness is observed nearly constant (~40 m). From the glacier bed topography, a sudden change in glacier depth is observed between observation points 14 and 19. These higher depth values may be

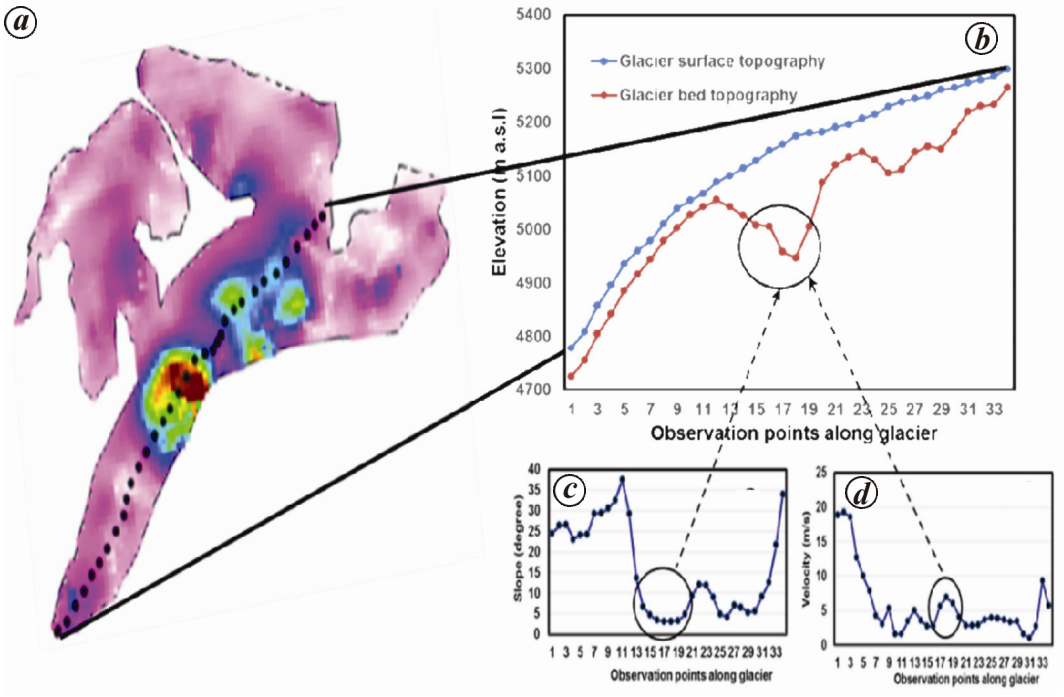

Figure 7. ***a***, Observation points along the centre of the Patseo glacier; ***b***, surface and bed topography of the glacier; ***c***, spatial variation of slope; ***d***, velocity along the profile.

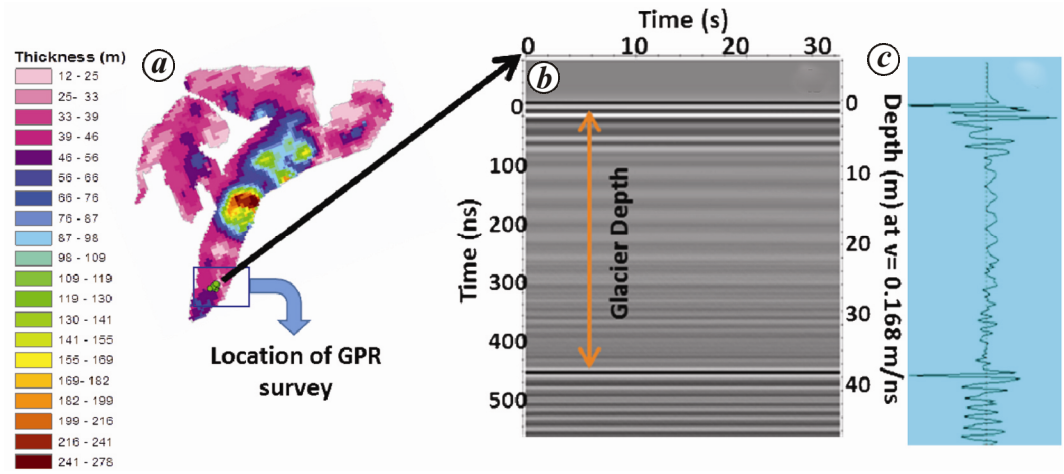

Figure 8. ***a***, Location of GPR survey; ***b***, radargram showing the glacier depth; ***c***, trace window depicting the individual trace.

attributed to the lower slope and higher velocity values (Figure 7 *c* and *d* respectively).

The ice-thickness map of the Patseo glacier was validated using GPR data, collected in 2013. As shown in Figure 8 *a*, GPR profiling was conducted using 40 MHz GPR antenna near the snout of the glacier. Figure 8 *b* and *c* show the radargram and trace window of the GPR data. The acquisition of data was carried out using EM wave velocity of 0.168 m/ns. At the survey site the ice was covered with moraine and thus directly using the EM wave velocity for ice may introduce error in the thickness estimation. However, here we have measured moraine depth at a number of places and the average depth was observed to be 40 cm. To estimate the glacier ice depth, we have subtracted this moraine cover depth from the total glacier depth.

From the radargram a sharp reflection was observed at 39 m depth and the same was also seen in the trace window (Figure 8 *c*), which showed a sudden change in the amplitude of the signal. This reflection from 39 m depth is from the interface between two different media, in this case from the bed surface of the glacier.

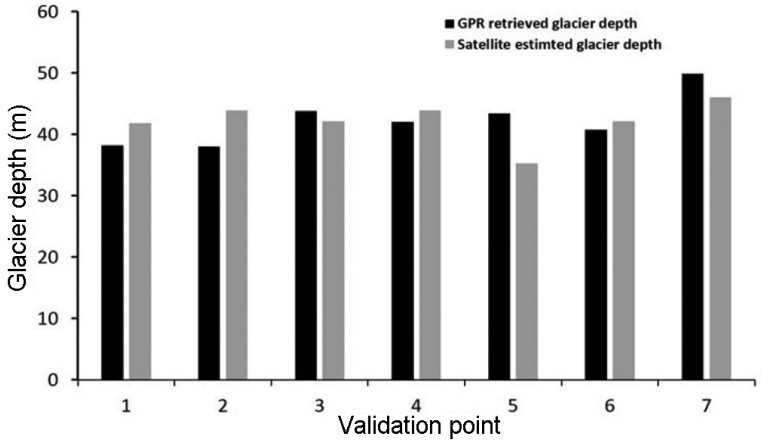

Figure 9. Comparison between GPR-retrieved and satellite data-estimated glacier depth values.

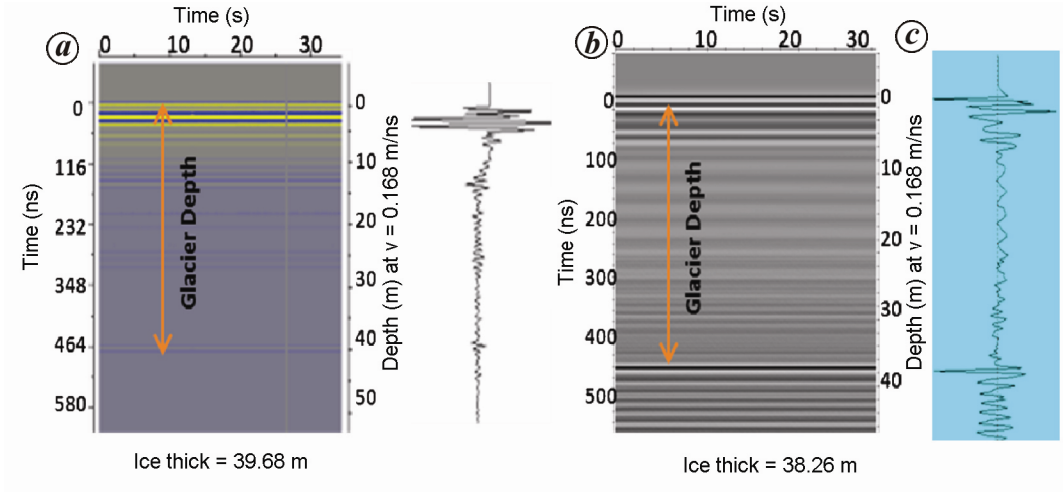

Figure 10. GPR profiles collected from the Patseo glacier during (***a***) 2004 and (***b***) 2013.

The GPR-measured glacier depth at some points was compared with the satellite data-estimated depth. The analysis revealed that the glacier depth values using GPR were close to satellite estimated values (Figure 9) with root mean square error (RMSE) of 4.75 m and mean absolute error (MAE) of 3.74 m. Hence this satellite data-based thickness map was further used to estimate the glacier ice volume. From our analysis estimated glacier ice volume was ~15.8×10^7 m^3 and its equivalent water reservoir was ~14.5×10^7 m^3.

The temporal change in glacier ice thickness is important to understand the mass and energy balance of the glacier. Figure 10 *a* and *b* shows the GPR profile collected from the same location of the Patseo glacier in 2004 and 2013. The analysis revealed that the glacier ice thickness at this particular location had reduced by ~1.42 m between 2004 and 2013. However, after analysing all the collected GPR profiles from various locations, it was observed that the average reduction in glacier depth was ~1.89 m between 2004 and 2013. This resulted in an annual ice thickness reduction of ~0.21 m.

Apart from the change in thickness, the areal change in the glacier was also estimated. Figure 11 shows the extent of the Patseo glacier in 2004 and 2013. The glacier area was estimated to be ~2.52 sq. km in 2004 and ~2.30 sq. km in 2013. An annual reduction of ~0.024 sq. km in the glacier area was also observed. Our study showed the total annual loss in glacier ice volume to be ~4.55×10^5 m^3.

Error in estimation of glacier thickness and area

Uncertainties in the estimation of glacier thickness and area may exists due to: (1) varying EM wave velocity in the ice media and (2) satellite-based glacier mapping. However, creep parameter, shape factor and slope angle may also introduce uncertainty in the glacier volume[13]. In the present study we have estimated the uncertainty in GPR-estimated glacier depth values and satellite data-based glacier areal extent. As already discussed, estimation of glacier depth using GPR depends on the dielectric

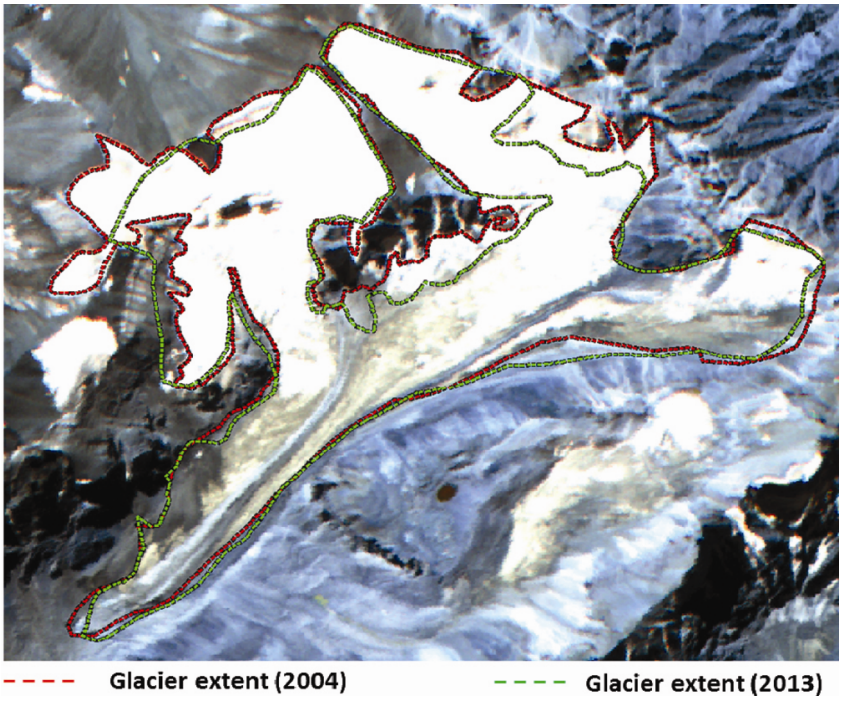

Figure 11. Areal extent of the Patseo glacier. Red and green colours indicate glacier extent in 2004 and 2013 respectively.

properties of the ice media. According to Ulaby *et al.*[23], the dielectric constant of glaciated ice varies between 3.14 and 3.18. In the present study, we have used dielectric constant value of 3.17 for GPR data processing. The corresponding EM wave velocity is 0.1679 m/ns. Maximum uncertainty in the glacier depth estimation may exist if the dielectric constant value of 3.14 is used for ice, which corresponds to wave velocity of 0.1687 m/ns. This uncertainty in velocity value, i.e. 0.1679 m/ns or 0.1687 m/ns will introduce an error of 0.86% in the glacier depth.

The uncertainty in glacier area mapping is estimated using eq. (6). From our analysis nearly 4200 pixels were found along the glacier boundary as observed from LISS IV satellite data. The estimated error in glacier mapping was found ±0.0706 sq. km, which is about 3.06% of the glacier area.

Conclusion

We have generated surface velocity map of the Patseo glacier using COSI-Corr technique. The study was carried out using Landsat 8 satellite images of 2014 and 2015. The average surface velocity of the glacier was observed to be ~5.47 m/year. Further, surface velocity along with slope and other ice parameters were used to generate the glacier ice-thickness distribution map. The average thickness of the glacier was estimated to be ~59 m. The spatial distribution of glacier depth and further assessment of glacier volume and stored water are essential to manage water resources of the Himalaya, and to also understand the impact of climate change. In the past various conventional methods, including volume–area relations have been used to determine the volume and stored water of glaciers. However, in most of these studies, validation was not done and hence the accuracy of the results could not be verified.

The present study has an advantage over other glacier depth/volume estimation methods, as here the validation of satellite data-estimated ice depth values is conducted using the GPR-measured ice depth. GPR survey was conducted in 2004 and 2013 to estimate ice thickness at some of the points near the snout of the glacier. Both the satellite data-retrieved and GPR-measured ice thickness values were found comparable. The total glacier ice volume was $\sim 15.8 \times 10^7$ m^3 with equivalent water reservoir $\sim 14.5 \times 10^7$ m^3 in 2015. Analysis of GPR profiles collected in 2004 and 2013, revealed an annual reduction of ~0.21 m in glacier ice thickness. Further, an annual decrease of ~0.024 sq. km in glacier area was found using the LISS IV satellite images. Another important outcome of this study is the estimation of annual loss in glacier ice volume, which was estimated as $\sim 4.55 \times 10^5$ m^3. Delineated bottom topography of the glacier in the present study is important to identify the probable glacier lake formations in the region. Due to hostile weather conditions during the survey, only a small area could be covered using GPR. Thus the validation of satellite-estimated glacier depth values was done only for a few point locations in the ablation zone of the glacier. In future, GPR profiling

may be conducted at various locations on the glacier, including the accumulation zone to estimate glacier volume and its stored water more accurately.

1. Oerlemans, J., Extracting climate signals from 169 glacier records. *Science*, 2005, **308**, 675–677.
2. Wagnon, P. *et al.*, Four years of mass balance on Chhota Shigri Glacier, Himachal Pradesh, India, a new benchmark glacier in the western Himalaya. *J. Glaciol.*, 2007, **53**, 603–611.
3. Kääb, A., Chiarle, M., Raup, B. and Schneider, C., Climate change impacts on mountain glaciers and permafrost. *Global Planet. Change*, 2007, **56**, vii–ix.
4. Tawde, S. A., Kulkarni, A. V. and Bala, G., Estimation of glacier mass balance on a basin scale: an approach based on satellite-derived snowlines and a temperature index model. *Curr. Sci.*, 2016, **111**(12), 1077–1989.
5. Joughin, I., Ice sheet velocity mapping: a combined interferometric and speckle-tracking approach. *Ann. Glaciol.*, 2002, **34**, 195–201.
6. Strozzi, T., Luckman, A., Maurray, T., Wegmuller, U. and Wener, C. I., Glacier motion estimation using SAR offset-tracking procedure. *IEEE Trans. Geosci. Remote Sensing*, 2002, **40**(11), 2384–2391.
7. Kimura, H., Kanamori, T., Wakabayashi, H. and Nishio, F., Ice sheet motion in inland Antarctica from JERS-1 SAR interferometry. *IEEE Int. Geosci. Remote Sensing*, 2004, **1–7**, 3018–3020.
8. Scambos, T. A. *et al.*, Application of image cross-correlation to the measurement of glacier velocity using satellite image data. *Remote Sensing Environ.*, 1992, **42**(3), 177–186.
9. Rolstad, C. *et al.*, Visible and near-infrared digital images for determination of ice velocities and surface elevation during a surge on Osbornebreen, a tidewater glacier in Svalbard. *Ann. Glaciol.*, 1997, **24**, 255–261.
10. Herman, F., Anderson, B. and Leprince, S., Mountain glacier velocity variation during a retreat/advance cycle quantified using sub-pixel analysis of ASTER images. *J. Glaciol.*, 2011, **57**(202), 197–207.
11. Leprince, S. *et al.*, Monitoring earth surface dynamics with optical imagery. *EOS Trans.*, 2008, **89**(1), 1–2.
12. Tiwari, R. K., Gupta, R. P. and Arora, M. K., Estimation of surface ice velocity of Chhota-Shigri glacier using sub-pixel ASTER image correlation. *Curr. Sci.*, 2014, **106**(6), 853–859.
13. Gantayat, P., Kulkarni, A. V. and Srinivasan, J., Estimation of ice thickness using surface velocities and slope: case study at Gangotri Glacier, India. *J. Glaciol.*, 2014, **60**(220), 277–282.
14. Negi, H. S., Saravana, G., Rout, R. and Snehmani, Monitoring of great Himalayan glaciers in Patsio region, India using remote sensing and climatic observations. *Curr. Sci.*, 2013, **105**(10), 1383–1392.
15. Leprince, S., Barbot, S., Ayoub, F. and Avouac, J. P., Automatic and precise orthorectification, coregistration, and subpixel correlation of satellite images, application to ground deformation measurements. *IEEE Trans. Geosci. Remote Sensing*, 2007, **45**(6), 1529–1558.
16. Farinotti, D., Huss, M., Bauder, A., Funk, M. and Truffer, M., A method to estimate ice volume and ice-thickness distribution of alpine glaciers. *J. Glaciol.*, 2009, **55**(191), 422–430.
17. Haeberli, W. and Hoelzle, M., Application of inventory data for estimating characteristics of and regional climate-change effects on mountain glaciers: a pilot study with the European Alps. *Ann. Glaciol.*, 1995, **21**, 206–212.
18. Kamb, B. and Echelmeyer, K. A., Stress-gradient coupling in glacier flow: I. Longitudinal averaging of the influence of ice thickness and surface slope. *J. Glaciol.*, 1986, **32**(111), 267–284.
19. Cuffey, K. M. and Paterson, W. S. B., *The Physics of Glaciers*, Butterworth-Heinemann, Oxford, 2010, 4th edn.
20. Jiracek, G. R. and Bentley, C. R., Velocity of electromagnetic waves in Antarctic ice. *Antarct. Res. Ser.*, 1971, **16**, 199–208.
21. Robin, G. D. E. Q., Velocity of radio waves in ice by means of a bore-hole interferometric technique. *J. Glaciol.*, 1975, **15**(73), 151–159.
22. Basnett, S., Kulkarni, A. V. and Bolch, T., The influence of debris cover and glacial lakes on the recession of glaciers in Sikkim Himalaya, India. *J. Glaciol.*, 2013, **59**(218), 1–12.
23. Ulaby, F. T., More, R. K. and Fung, A. K., *Microwave Remote Sensing: Active and Passive*. Volume III from Theory to Applications, Artech House, Inc, USA, 1986.

ACKNOWLEDGEMENTS. We thank the US Geological Survey for its free data policy, allowing us to use Landsat images and ASTER DEM for analysis. We also thank S. Leprince, S. Barbot, F. Ayoub and J. P. Avouac for providing the COSI-Corr module freely on the internet.

doi: 10.18520/cs/v114/i04/776-784